AMERICAN SOCIETY FOR MICROBIOLOGY | Journal of Virology®

VACCINES AND ANTIVIRAL AGENTS

# Targeting Conserved Sequences Circumvents the Evolution of Resistance in a Viral Gene Drive against Human Cytomegalovirus

Marius Walter,[a] Rosalba Perrone,[a] Eric Verdin[a]

[a]Buck Institute for Research on Aging, Novato, California, USA

**ABSTRACT** Gene drives are genetic systems designed to efficiently spread a modification through a population. They have been designed almost exclusively in eukaryotic species, especially in insects. We recently developed a CRISPR-based gene drive system in herpesviruses that relies on similar mechanisms and could efficiently spread into a population of wild-type viruses. A common consequence of gene drives in insects is the appearance and selection of drive-resistant sequences that are no longer recognized by CRISPR-Cas9. In this study, we analyzed in cell culture experiments the evolution of resistance in a viral gene drive against human cytomegalovirus. We report that after an initial invasion of the wild-type population, a drive-resistant population is positively selected over time and outcompetes gene drive viruses. However, we show that targeting evolutionarily conserved sequences ensures that drive-resistant viruses acquire long-lasting mutations and are durably attenuated. As a consequence, and even though engineered viruses do not stably persist in the viral population, remaining viruses have a replication defect, leading to a long-term reduction of viral levels. This marks an important step toward developing effective gene drives in herpesviruses, especially for therapeutic applications.

**IMPORTANCE** The use of defective viruses that interfere with the replication of their infectious parent after coinfecting the same cells—a therapeutic strategy known as viral interference—has recently generated a lot of interest. The CRISPR-based system that we recently reported for herpesviruses represents a novel interfering strategy that causes the conversion of wild-type viruses into new recombinant viruses and drives the native viral population to extinction. In this study, we analyzed how targeted viruses evolved resistance against the technology. Through numerical simulations and cell culture experiments with human cytomegalovirus, we showed that after the initial propagation, a resistant viral population is positively selected and outcompetes engineered viruses over time. We show, however, that targeting evolutionarily conserved sequences ensures that resistant viruses are mutated and attenuated, which leads to a long-term reduction of viral levels. This marks an important step toward the development of novel therapeutic strategies against herpesviruses.

**KEYWORDS** gene drive, biotechnology, cytomegalovirus, drug resistance evolution, herpesviruses, viral interference

Herpesviruses are nuclear-replicating viruses with large double-stranded DNA genomes (100 to 200 kb) that include hundreds of genes (1). They establish lifelong persistent infections and are implicated directly or indirectly in numerous human diseases (2). In particular, human cytomegalovirus (hCMV) is an important threat to immunocompromised patients, such as HIV-infected individuals, recipients of organ transplants, and fetuses.

**Citation** Walter M, Perrone R, Verdin E. 2021. Targeting conserved sequences circumvents the evolution of resistance in a viral gene drive against human cytomegalovirus. J Virol 95: e00802-21. https://doi.org/10.1128/JVI.00802-21.

**Editor** Felicia Goodrum, University of Arizona



Address correspondence to Marius Walter, mwalter@buckinstitute.org, or Eric Verdin, everdin@buckinstitute.org.

**Received** 11 May 2021
**Accepted** 13 May 2021
**Accepted manuscript posted online** 19 May 2021
**Published** 12 July 2021

The use of defective viruses that interfere with the replication of their infectious parent after coinfecting the same cells—a therapeutic strategy known as viral interference—has generated a lot of interest in recent years. Different strategies against HIV or influenza or Zika virus have been described (3–5). The viral gene drive system that we recently reported for herpesviruses (with hCMV) represents a novel interfering strategy that causes the conversion of wild-type viruses into new recombinant viruses and drives the native viral population to extinction (6). Gene drives are genetic modifications designed to spread efficiently in a target population (7–10). They have been engineered principally in insect species, such as mosquitoes, and are seen as a potential strategy to eradicate vector-borne diseases, such as malaria and dengue. Most gene drives rely on CRISPR-mediated homologous recombination and have been restricted to sexually reproducing organisms. The viral gene drive system that we developed with hCMV relies on coinfection of cells by a wild-type and an engineered virus (6). Cleavage by Cas9 and repair by homologous recombination lead to the conversion of wild-type viruses into new recombinant viruses (Fig. 1A). We demonstrated that gene drive viruses can replace their wild-type counterparts and spread in the viral population in cell culture experiments. Moreover, we showed that a gene drive virus presenting severe replicative defects could spread into the viral population and ultimately reduce viral levels. This development represents a novel therapeutic strategy against herpesviruses.

An important challenge lies in designing gene drive viruses with replicative defects that still spread efficiently in the viral population and ultimately reduce viral levels. In the ideal scenario, gene drive viruses are noninfectious but are complemented by wild-type factors upon coinfection and can spread in the population only as long as wild-type viruses are present. Our initial study targeted *UL23*, a viral gene that encodes a tegument protein involved in immune evasion. UL23 is dispensable under normal cell culture conditions but necessary in the presence of interferon gamma (6, 11, 12). The tegument of herpesvirus is a layer of protein that lies between the genome-containing capsid and the viral envelope (1, 13). Tegument proteins are released in the cell upon viral entry and are often involved in transcriptional activation and immune evasion. Tegument proteins are attractive targets for a viral gene drive because many of them function early in the viral cycle—when they could be complemented by a coinfecting wild-type virus—but accumulate only during later stages of the infection. In the present study, we designed gene drives against several tegument genes and showed that they indeed represent effective targets.

An important aspect of gene drive in sexually reproducing organisms, such as mosquitoes, is the appearance and selection of drive-resistant alleles that are no longer recognized by the CRISPR guide RNA (gRNA) (14–16). Such alleles can already exist in the wild population or appear when the target site is repaired and mutated by nonhomologous end joining instead of homologous recombination (Fig. 1A). These sequences are "immune" to future conversion into the drive allele, are often positively selected over time, and limit the ability to permanently modify a wild-type population (16–19).

In this study, we investigated the appearance and evolution of resistance in a viral gene drive. Through numerical simulations and cell culture experiments with hCMV, we showed that after the initial propagation, a drive-resistant viral population is positively selected and outcompetes gene drive viruses over time. By designing and testing multiple gene drives that disable critical viral genes, we showed that targeting evolutionarily conserved sequences ensures that drive-resistant viruses have a replication defect that leads to a long-term reduction of viral levels.

## RESULTS

**Drive-resistant viruses are positively selected over time.** We first attempted to model the evolution of gene drive resistance using numerical simulations. Our initial study indicated that after the successful propagation of the gene drive in the wild-type

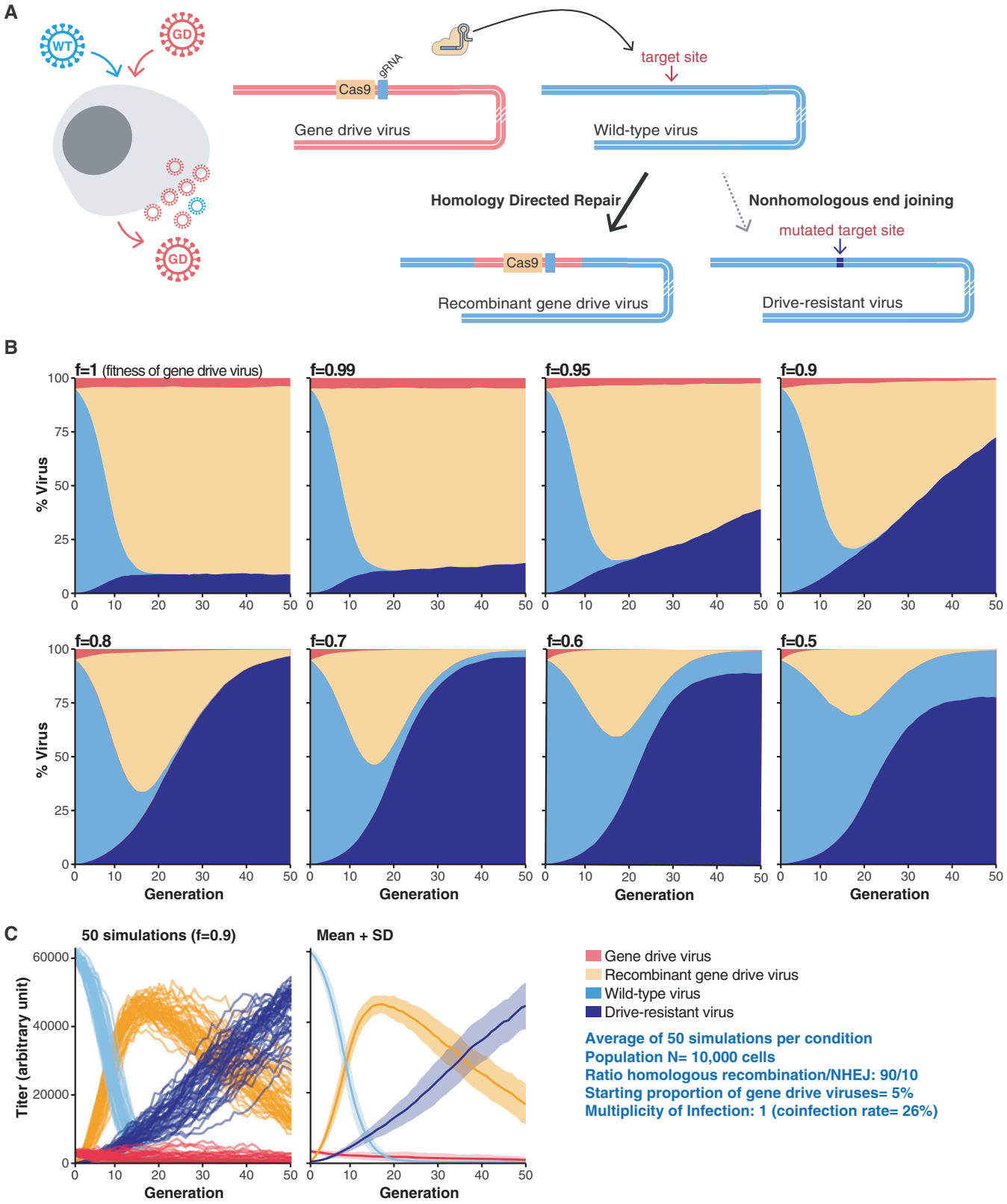


**FIG 1** Evolution of gene drive resistance in numerical simulations. (A) CRISPR-based gene drive sequences are, at a minimum, composed of Cas9 and a gRNA targeting the complementary wild-type locus. After coinfection of a cell by a wild-type (WT) and a gene drive (GD) virus, Cas9 targets and cleaves the wild-type sequence. Homology-directed repair of the damaged wild-type locus using the gene drive sequence as a repair template causes the conversion of the wild-type locus into a new gene drive sequence and the formation of new recombinant viruses. In 5 to 10% of cases, repair of the

(Continued on next page)

population, around 5 to 10% of viruses had accumulated mutations of the target site. These mutations were caused by nonhomologous repair of the cleavage site and rendered the mutated viruses resistant to the drive (6). Using a 10% estimate and considering in this scenario that resistant viruses would replicate at the same level as the wild type, we modeled the evolution of the viral population over time (Fig. 1B and C). These simulations showed that depending on the replicative fitness of gene drive viruses, a population of drive-resistant viruses is often positively selected over time. At low fitness cost, the gene drive virus first spreads efficiently in the wild-type population but is outcompeted in the long run. At high fitness cost, a resistant population appears quickly and gene drive viruses disappear rapidly. Overall, these simulations predict that the appearance of drive-resistant viruses would prevent the gene drive from permanently remaining in the viral population.

We next evaluated experimentally the evolution of resistance in cell culture. Our initial experimental system involved an unmodified hCMV expressing green fluorescent protein (GFP) (strain Towne, referred to here as Towne-GFP) and an mCherry-expressing gene drive virus (GD-UL23) targeting *UL23* (6) (Fig. 2A). *UL23* is dispensable under normal cell culture conditions (11, 12), but the GD-UL23 virus was built in a different viral strain (TB40/E) and replicated significantly slower than Towne-GFP ($P = 0.0011$, Welsh *t* test on log-transformed data [Fig. 2B]). Human foreskin fibroblasts were coinfected at a low multiplicity of infection (MOI; 0.1) with the two viruses in different starting proportions, and the infection was subsequently propagated for several weeks by infecting fresh cells every 10 to 15 days. The MOI was kept around 0.1 at each passage. The proportion of the different viruses was evaluated over time by plaque assay (Fig. 2C and D). The mCherry reporter enabled us to follow the spread of the gene drive in the viral population: viruses expressing mCherry represent gene drive viruses, and viruses expressing only GFP are unconverted—either unmodified or drive-resistant—viruses. In each of 12 biological replicates and independently of the starting proportion of GD-UL23, wild-type viruses were first converted to new gene drive viruses, and the population of GFP-only viruses reached a minimum level of 5 to 40% after 10 to 40 days (Fig. 2C). In a second phase, however, GFP-only viruses appeared to be positively selected, and their proportion rebounded until they represented the majority of the viral population. This showed that in the long term, drive-resistant viruses are positively selected.

These first experiments were carried out with two viruses from different strains, which complicated the interpretation of the results. To alleviate the influence of the viral strain, we analyzed the evolution of resistance in a strict Towne background. Two gene drive plasmids (with a gRNA targeting either the *UL23* 5′ untranslated region (UTR) or *UL23* start codon) were separately transfected into fibroblasts, and cells were subsequently infected with Towne-eGFP. The population of mCherry-expressing recombinant viruses and of GFP-only (unmodified or resistant) viruses was followed over time. As observed previously, the gene drive cassette spread efficiently until the population of GFP-only viruses reached a minimum after 70 days (Fig. 3A). Introduction of a cassette in the viral genome by transfection of a plasmid is a notoriously inefficient process. It was nonetheless sufficient to generate enough recombinant gene drive viruses to enable propagation of the gene drives through the viral population, which further demonstrated the high efficiency of the system. Importantly, directly transfecting a plasmid circumvented the time-consuming process of generating and purifying recombinant viruses, allowing testing of multiple gene drive constructs in parallel. The population of drive-resistant viruses at 70 days was characterized by amplicon

**FIG 1** Legend (Continued)
damaged genome by nonhomologous end joining (NHEJ) creates drive-resistant viruses with a mutated target site. (B) Numerical simulation showing that the appearance and positive selection of drive-resistant viruses depend on the replicative fitness *f* of gene drive viruses. In these simulations, at each viral generation, *N* virtual cells were randomly infected and coinfected by *N* viruses, producing a new generation of viruses. When a cell is coinfected by wild-type and gene drive viruses, wild-type viruses are converted to new gene drive viruses or resistant viruses in a 90/10 ratio. (C) Example of a simulation with a replicative fitness *f* of 0.9 for gene drive viruses. The left graph shows 50 independent simulations. The right graph shows the mean and standard deviation of the 50 simulations. NHEJ, nonhomologous end joining.

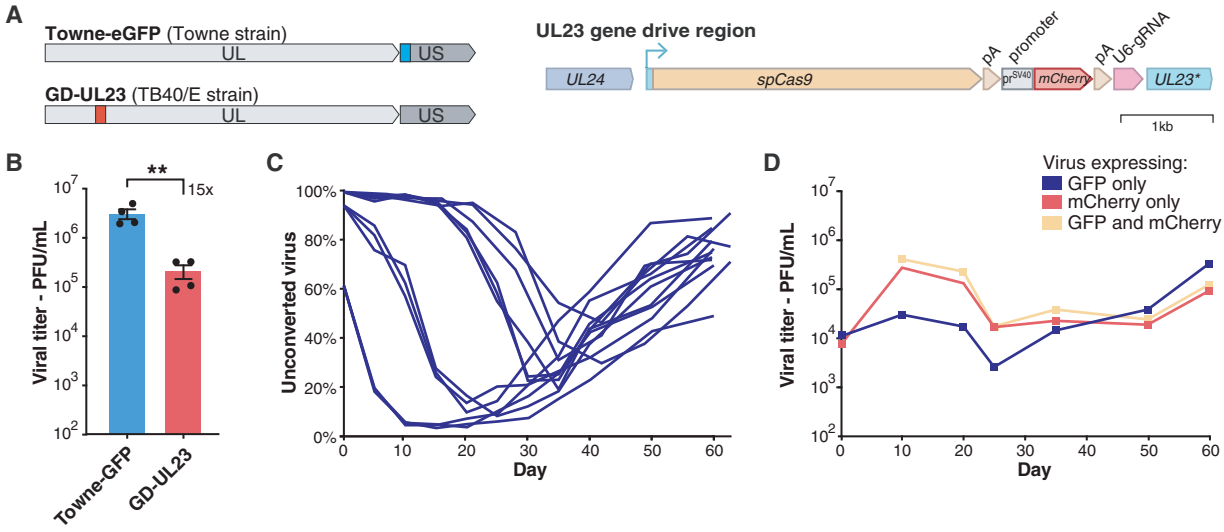


**FIG 2** Evolution of resistance in a gene drive against UL23. (A) (Left) Localizations of gene drive and GFP cassettes on hCMV genomes. UL and US, unique long and short genome segments. (Right) the gene drive cassette comprises *SpCas9* under the control of the *UL23* endogenous promoter, followed by a simian virus 40 (SV40) poly(A) signal, an SV40 promoter driving an mCherry reporter, a beta-globin poly(A) signal and a U6-driven gRNA. (B) Viral titer in fibroblasts infected with Towne-GFP or GD-UL23 viruses after 7 days, as measured by plaque assay. MOI = 1; $n = 4$. **, $P < 0.01$, Welsh $t$ test on log-transformed data. (C) Proportion over time of unconverted viruses expressing only GFP after coinfection with Towne-GFP and GD-UL23, as measured by plaque assay (MOI = 0.1 at day 0). Every line corresponds to a biological replicate ($n = 12$), with different starting proportions of GD-UL23: 40%, 10%, 1%, or 0.1%, at 3 replicates per starting condition. (D) Viral titers over time of viruses expressing GFP alone, mCherry alone, or both, after coinfection with Towne-GFP and GD-UL23. This panel corresponds to the starting proportion of 40% that is shown in panel C. $n = 3$. Data show means and SEM between biological replicates. Titers are expressed in PFU (plaque-forming units) per mL of supernatant.

sequencing of the target site, in three biological replicates for the two conditions (Fig. 3B to D). As expected, the target site was heavily mutated, with up to 98% of sequences modified in some of the replicates (Fig. 3C). Interestingly, around 80% of sequences edited with gRNA-5′ UTR had the same 3-bp deletion. In contrast, edits generated by gRNA-ATG were more diverse, with a dominant 2-bp deletion (Fig. 3D). These results confirmed that drive-resistant viruses accumulate over time, limiting the impact of the drive.

Finally, we isolated and purified a gene drive virus against *UL23* in a Towne strain ($GD^{Towne}$-UL23). Fibroblasts were coinfected with Towne-GFP and $GD^{Towne}$-UL23 (MOI = 1), and the population of unconverted viruses expressing only GFP was analyzed over time (Fig. 3E and F). Cells were infected with a starting proportion of $GD^{Towne}$-UL23 of 1 to 2%, and the infection was propagated for several weeks by infecting fresh cells every 7 to 8 days (MOI around 1 at each passage). In this experiment, the drive achieved more than 99% penetrance in the viral population, and the proportion of unconverted viruses only rebounded slightly and plateaued at around 10 to 20% (Fig. 3E). UL23 is dispensable under normal cell culture conditions (6, 11), and viral titers remained constant over the course of the experiment (Fig. 3F). This result showed that a gene drive without fitness cost can stably invade the wild-type population, as predicted by numerical simulations.

These numerical and experimental results indicate that after the initial invasion of the wild-type population, a drive-resistant viral population is positively selected over time and outcompetes gene drive viruses. Importantly, however, we showed that in the absence of associated fitness costs, gene drive sequences can reach almost full penetrance and be maintained durably in the viral population.

**Gene drives against conserved regions of *UL26* and *UL35* spread efficiently in the viral population.** We next sought to design gene drives that would lead to a long-term reduction of viral levels. Drive-resistant viruses are created by imperfect repair of the CRISPR cleavage site. We reasoned that the appearance and selection of drive-resistant viruses could be circumvented if the mutation rendered viruses nonfunctional,

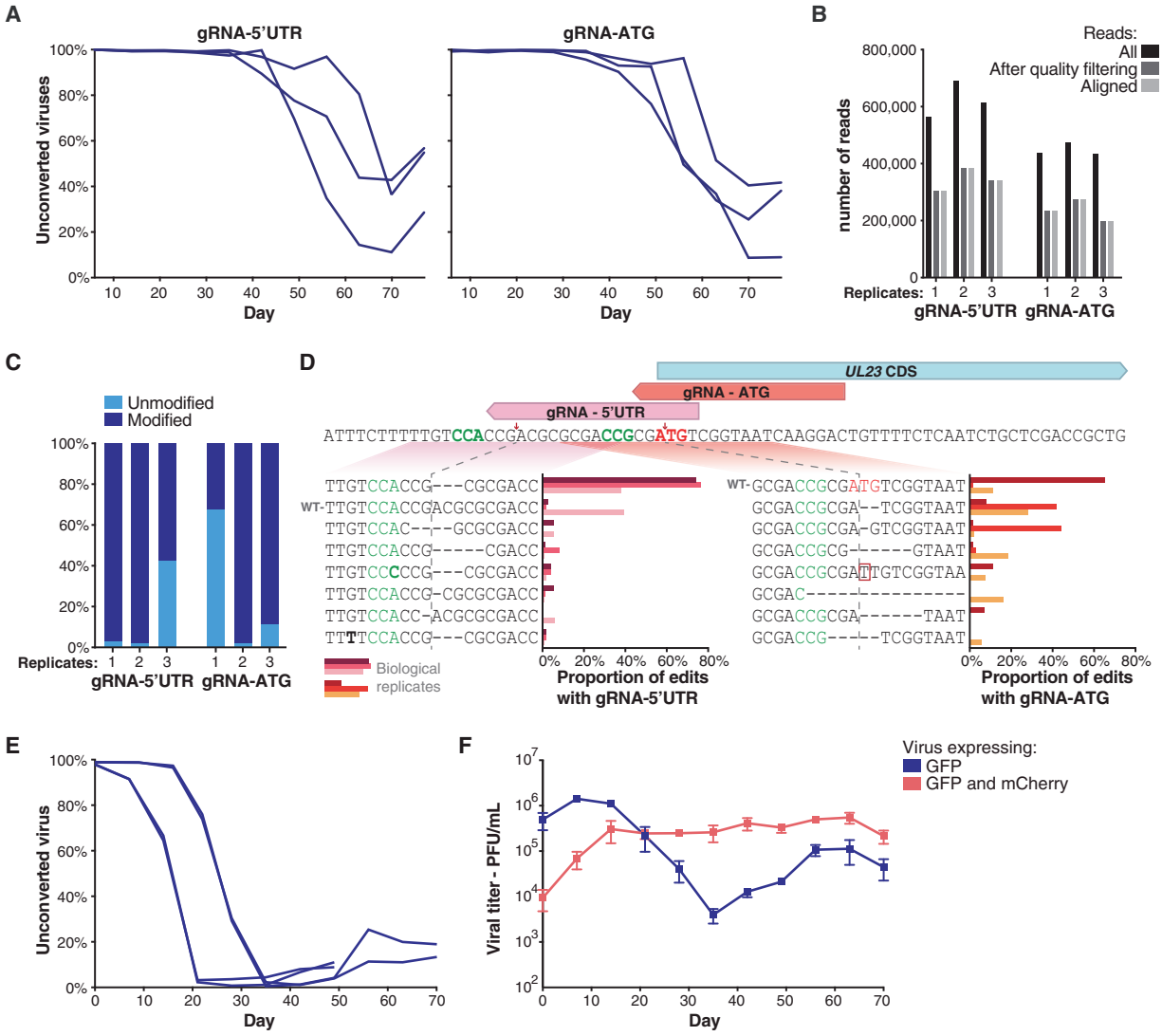


**FIG 3** Drive-resistant sequences are heavily mutated. (A) Proportion over time of viruses expressing only GFP in a gene drive against the *UL23* 5′ UTR or ATG. Fibroblasts were initially transfected with a gene drive plasmid against the UL23 5′ UTR or UL23 start codon and subsequently infected with Towne-GFP. (B to D) Amplicon sequencing of the CRISPR target site at the end of the drive (day 70). (B) Sequencing statistics; (C) proportion of edited genomes; (D) relative contribution of each edit. CRISPR cleavage sites are indicated by a red arrow, protospacer adjacent motifs (PAM) are highlighted in green, and the *UL23* start codon is in red. $n = 3$. (E and F) Proportion over time of viruses expressing only GFP (E) and viral titers (F) after coinfection with Towne-GFP and GD$^{Towne}$-UL23. MOI = 1 at day 0; $n = 4$. Data show means and SEM between biological replicates.

for example, if it knocked out a critical viral gene. In this case, numerical simulations predicted that drive-resistant viruses would also be counterselected and would not accumulate (Fig. 4), leading to a long-term reduction of viral titers. We therefore designed several gene drives targeting hCMV genes that are necessary for efficient viral replication (summary in Table 1). The gene drive cassette was inserted into the coding sequence of the viral gene. In addition, CRISPR gRNAs were designed in evolutionarily conserved sequences, so that any mutation would potentially affect viral fitness. In this situation, both gene drive and drive-resistant viruses would have a replication defect, leading to a long-term reduction of viral levels.

We first attempted to build gene drive viruses against *UL122* (IE2), *UL79*, *UL99*, and *UL55* (gB), using fibroblasts stably expressing the different viral genes. These viral genes are essential for viral replication and mutant viruses are noninfectious (20–24). We could generate gene drive viruses against *UL79* and *UL99* in complementing cells,

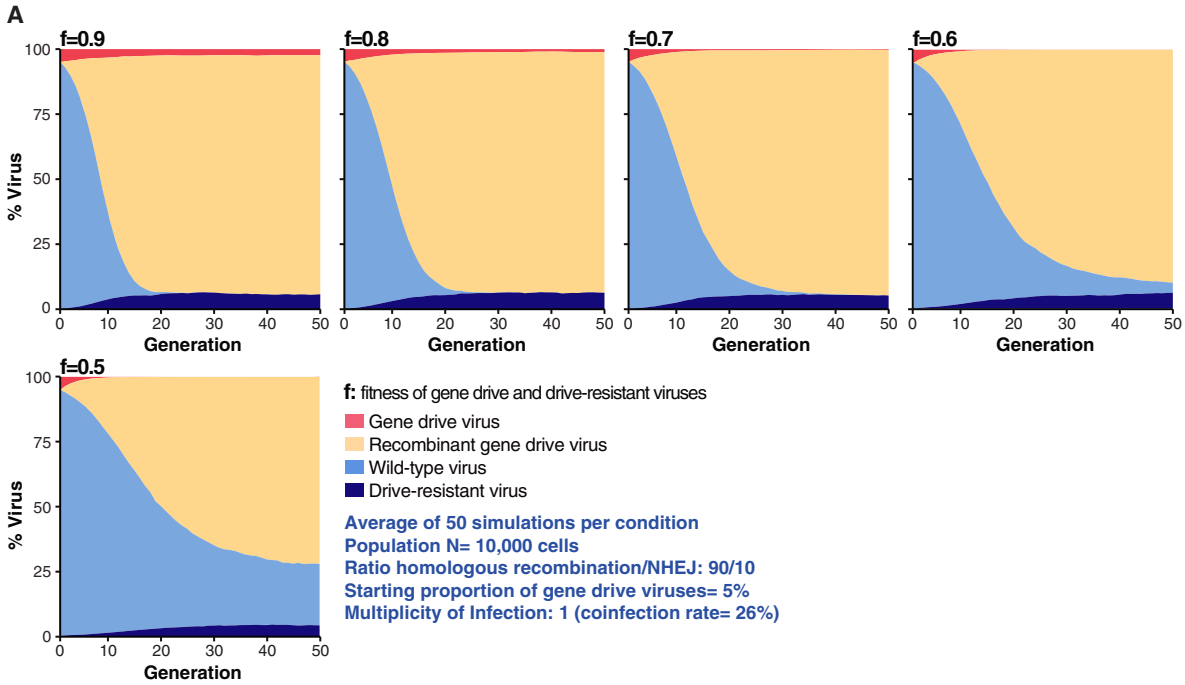


**FIG 4** Numerical simulation with gene drive and drive-resistant viruses having the same fitness *f*. In this model, drive-resistant viruses have no competitive advantage over gene drive viruses. In these simulations, at each viral generation, *N* virtual cells were randomly infected and coinfected by *N* viruses, producing a new generation of viruses. When a cell was coinfected by wild-type and gene-drive viruses, wild-type viruses were converted to new gene drive viruses or resistant viruses in a 90/10 ratio.

but we observed only a very few second-generation recombinant viruses when coinfecting with unmodified Towne-GFP. We were not able to build gene drive viruses against *IE2* and gB, in part because we did not succeed in generating fibroblasts stably expressing these two proteins. We also transfected fibroblasts with each individual plasmid before infecting cells with Towne-GFP virus, but we once again did not observe any recombinant viruses. These first attempts were unsuccessful, which suggested that coinfection with Towne-GFP was not sufficient to rescue these very strong

**TABLE 1** Summary of gene drive experiments against several viral genes

| Gene | Function | Phenotype | Ability to drive |
|---|---|---|---|
| *UL23* | Tegument gene involved in evasion of the innate immune response (11) | Dispensable (11) | Drives efficiently, up to 99% of conversion |
| *UL122* | Encodes immediate early protein IE2; responsible for the initiation of viral replication (20) | Essential (20) | Does not drive; no recombinant viruses could be observed |
| *UL79* | Regulation of transcription of late viral transcripts (21) | Essential (22) | Does not drive; very few recombinant viruses |
| *UL99* | Tegument gene essential for viral envelopment (23) | Essential (23) | Does not drive; no recombinant virus |
| *UL55* | Encodes fusion protein gB | Essential (24) | Does not drive; no recombinant virus |
| *UL26* | Tegument gene involved in immune evasion, transcriptional activation and virion stability (25, 29–31) | Severe growth defect (25) | Drives efficiently |
| *UL35* | Tegument gene important for viral replication and virion formation (52) | Moderate growth defect (26) | Drives efficiently |
| *UL69* | Tegument gene involved in unspliced mRNA nuclear export and cellular arrest (27, 53) | Severe growth defect (27) | Very limited drive at high MOI |
| *UL82* | Tegument gene that stimulates immediate-early transcription and inhibits host innate response (28, 47) | Moderate growth defect (28) | Very limited drive at high MOI |

loss-of-function mutants (Table 1). We next sought to target viral genes that are not absolutely essential but still required for efficient viral replication. As explained in the introduction, we hypothesized that tegument proteins represented attractive targets. We designed gene drive plasmids against the tegument genes *UL26*, *UL35*, *UL69*, and *UL82*, which, when mutated or deleted, lead to moderate growth defects (25–28). Fibroblasts were independently transfected with each individual plasmid and infected with Towne-GFP virus (MOI = 1) and the population of recombinant viruses was followed over time (Table 1). We observed that the constructs against *UL26* and *UL35* could spread in the wild-type population, and these genes were selected for subsequent experiments.

CRISPR gRNAs against *UL26* and *UL35* were chosen in sequences evolutionarily conserved at the DNA and amino acid levels. UL26 is a tegument protein involved in immune evasion, transcriptional activation, and virion stability (25, 29–31). It is a member of the US22 family of herpesviral proteins (32), a family of proteins with conserved motifs across several herpesviruses. We aligned 31 protein sequences of US22 family members and screened for conserved motifs (Fig. 5A). Two highly conserved motifs were found, and we chose to design a gRNA that would disrupt a very conserved proline in the second motif. In parallel, available DNA sequences for 235 hCMV clinical and laboratory viruses were aligned, and the frequency of variants compared to the Towne reference was calculated (Fig. 5B). The gRNA against *UL26* was chosen in a region of low variation, with less than 1% of sequenced hCMV viruses having a polymorphism in the first 18 bp of the gRNA sequence. A highly variable site was found in the gRNA sequence, but at a position (the 19th base) that presumably does not efficiently prevent DNA cleavage (33). Most repairs of the predicted cut site would disrupt the evolutionarily conserved proline. The gene drive cassette comprised *Cas9*, an mCherry reporter, and a U6-driven gRNA (Fig. 5C and D). Because the CRISPR target site against *UL26* was located far from the start codon (around 200 bp), a polyadenylation signal and a promoter with late kinetics (from hCMV *UL99*) were added to the gene drive cassette upstream of *Cas9*. The gRNA against *UL35* was designed in a similar manner. *UL35* encodes two isoforms with a common C-terminal domain but different N termini (26, 34). Mutant viruses lacking the longer isoform have a modest replicative defect, and the gRNA against *UL35* targeted this first start codon, so that any mutations at the predicted cut site would abrogate translation of the long isoform (Fig. 5D to F). This gRNA could not be designed in a region of low genetic variation (Fig. 5E). This finding has little consequence for cell culture experiments but suggests that this particular gene drive virus could be less efficient at targeting clinical hCMV strains.

Infectious gene drive viruses against *UL26* and *UL35* (GD-UL26 and GD-UL35, in strain Towne) were isolated and purified in fibroblasts. Of note, mutants lacking UL26 have severe growth defects (25) and the isolation and plaque assay of GD-UL26 viruses were carried out in cells stably expressing UL26. In wild-type fibroblasts, GD-UL26 replication was almost completely abrogated compared to that of Towne-GFP, while GD-UL35 replicated with a more moderate but significant 9-fold growth defect ($P < 0.0001$ and $P = 0.0039$, respectively, by analysis of variance [ANOVA] on log-transformed data [Fig. 6A]). GD-UL35 viral plaques were also significantly smaller than those of Towne-GFP, with a median plaque size 30% smaller ($P = 0.0003$, Mann-Whitney test [Fig. 6B]).

To analyze the long-term evolution of a gene drive against *UL26* and *UL35*, fibroblasts were coinfected with Towne-GFP and either GD-UL26 or GD-UL35 in a 99%/1% ratio and compared to cells infected with only Towne-GFP (MOI = 1). Viral titers and the population of unconverted GFP-only viruses representing unmodified or drive-resistant viruses were followed over time in four or eight independent replicates (Fig. 6C to E). In both situations and similar to the case with previous experiments, the drive first spread efficiently and the proportion of GFP-only viruses reached a minimum of around 20% (for GD-UL35) or 50% (for GD-UL26). In a second phase that corresponded to the positive selection of drive-resistant viruses, the population of GFP-only viruses

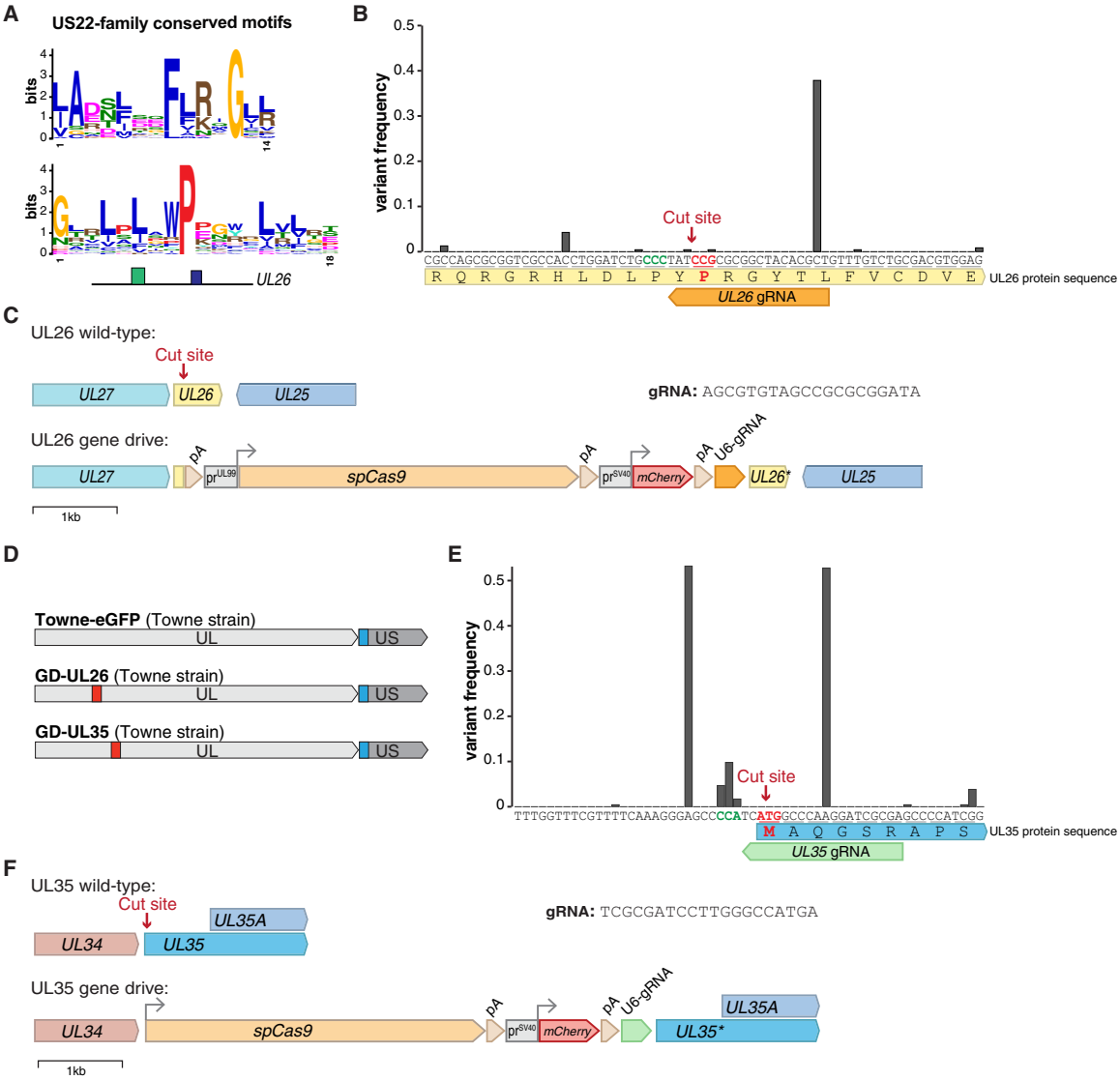


**FIG 5** Design of gene drives against UL26 and UL35. (A) Logo sequences of the two most conserved motifs in the US22 family of herpesviral proteins. At the bottom is shown the localization of the two motifs on UL26 protein (blue, first motif; green, second motif). (B) Frequency of genetic variants around the *UL26* target site, from 235 hCMV strains. The CRISPR PAM is highlighted in green, and the targeted proline codon is in red. (C) Wild-type and gene drive *UL26* regions. The gene drive cassette comprises a herpes simplex virus 1 thymidine kinase (HSV1-TK) poly(A) signal and *SpCas9* under the control of an *UL99* late viral promoter, followed by an SV40 poly(A) signal, an SV40 promoter driving an mCherry reporter, a beta-globin poly(A) signal, and a U6-driven gRNA. (D) Localizations of gene drive and GFP cassettes on hCMV genomes. (E) Frequency of genetic variants around the *UL35* target site, from 235 hCMV strains. The CRISPR PAM is highlighted in green, and the targeted start codon is in red. (F) Wild-type and gene drive *UL35* region. The gene drive cassette is the same as in panel C, except that *SpCas9* expression is controlled by the *UL35* endogenous promoter.

rebounded and gene drive viruses ultimately represented only a small fraction of the population. Notably, viral titers dropped importantly when the drive reached its maximum, around 100-fold in both cases. This finding confirmed our previous observation that a gene drive with moderate or severe replicative defects could spread in the viral population and that it could cause an important, albeit transient, reduction of viral titers. Viral levels then increased concomitantly to the rebound of the GFP-only population but remained 2- to 5-fold lower until the end of the experiment than for cells infected with only Towne-GFP (dashed line in Fig. 6D and E). As this remaining population likely represented drive-resistant viruses with a mutated target site, this

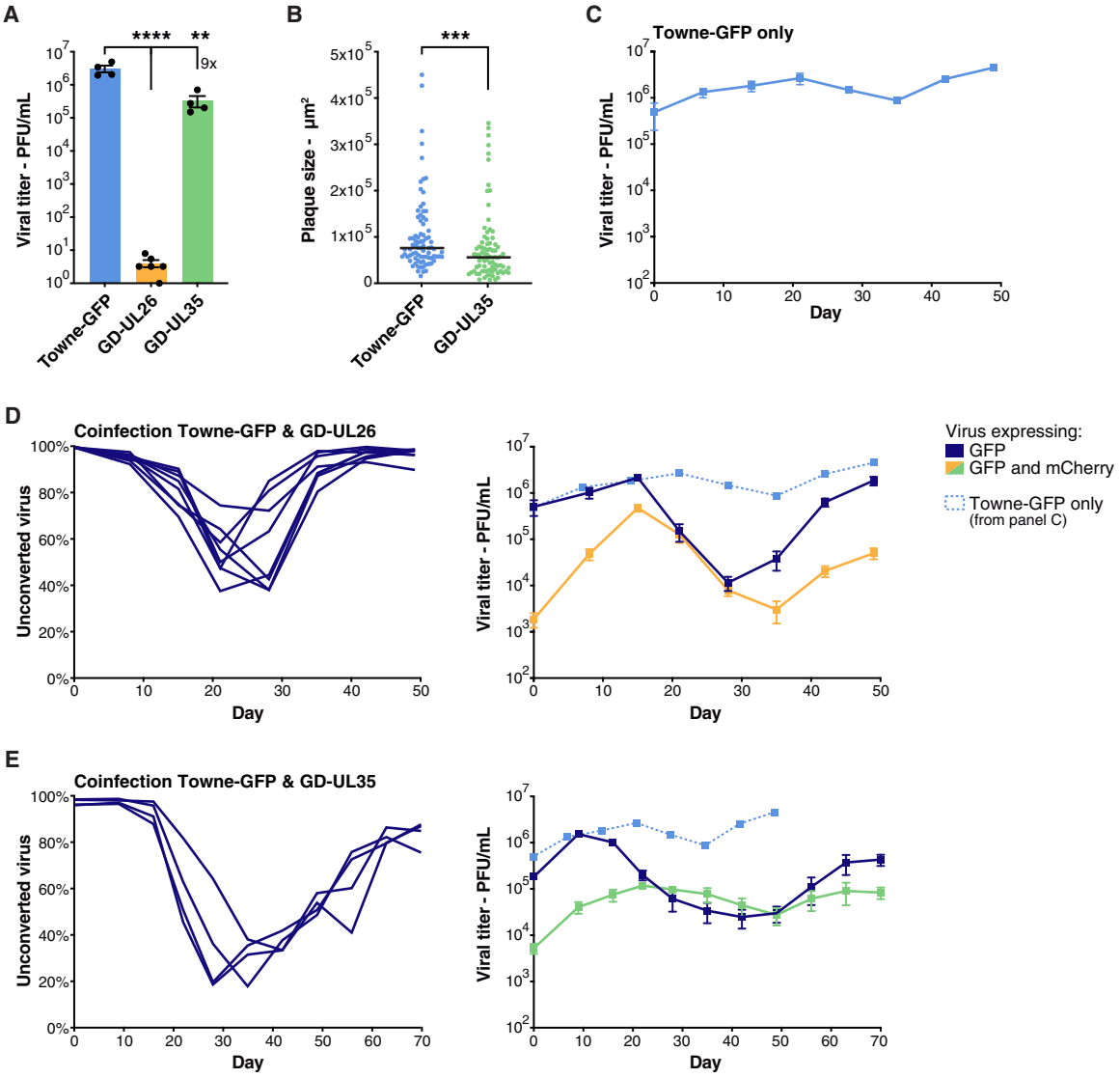


**FIG 6** Gene drives against *UL26* and *UL35* spread in the viral population. (A) Viral titer in fibroblasts infected with Towne-GFP, GD-UL26, or GD-UL35 virus after 7 days. MOI = 1; $n = 4$. (B) Plaque size in fibroblasts infected with Towne-GFP or GD-UL35, after 8 days. Black lines indicate the median; $n = 80$. (C) Viral titer over time in fibroblasts infected with Towne-GFP. At each time point, supernatant was used to infect fresh cells to propagate the infection. MOI = 1; $n = 4$. (D and E) (Left graphs) Proportion of the viral population expressing only GFP, representing unconverted (unmodified or drive-resistant) viruses, after coinfection with Towne-GFP and GD-UL26 (D) or GD-UL35 (E). (Right graphs) Viral titers over time. Viruses expressed either GFP only (dark blue) or both GFP and mCherry (yellow/green). Viruses expressing mCherry represent gene drive viruses. Results from panel C showing monoinfection with Towne-GFP are superposed (light blue). $n = 8$ (GD-UL26) or $n = 4$ (GD-UL35). MOI was kept around 1 to 2 at each passage. Data show mean and SEM between biological replicates. Asterisks summarize the results of statistical tests. **, $P < 0.01$; ***, $P < 0.001$; ****, $P < 0.0001$ (A, one-way ANOVA with Dunnett's T3 multiple-comparison test on log-transformed data; B, Mann-Whitney test).

observation suggested that drive-resistant viruses might have acquired a permanent replicative defect.

**Drive-resistant viruses are durably attenuated.** To investigate the population of drive-resistant viruses, viral clones resistant to either GD-UL26 or GD-UL35 and originating from three independent coinfection experiments were isolated and purified. PCR and Sanger sequencing of 11 viral clones for each condition revealed that the target site was mutated as expected (Fig. 7A and B). For *UL26*, six clones had an out-of-frame mutation that would disrupt translation, and the five others had an in-frame mutation that nonetheless mutated the conserved proline. On the other hand, every clone resistant to GD-UL35 had a mutated start codon that would prevent translation

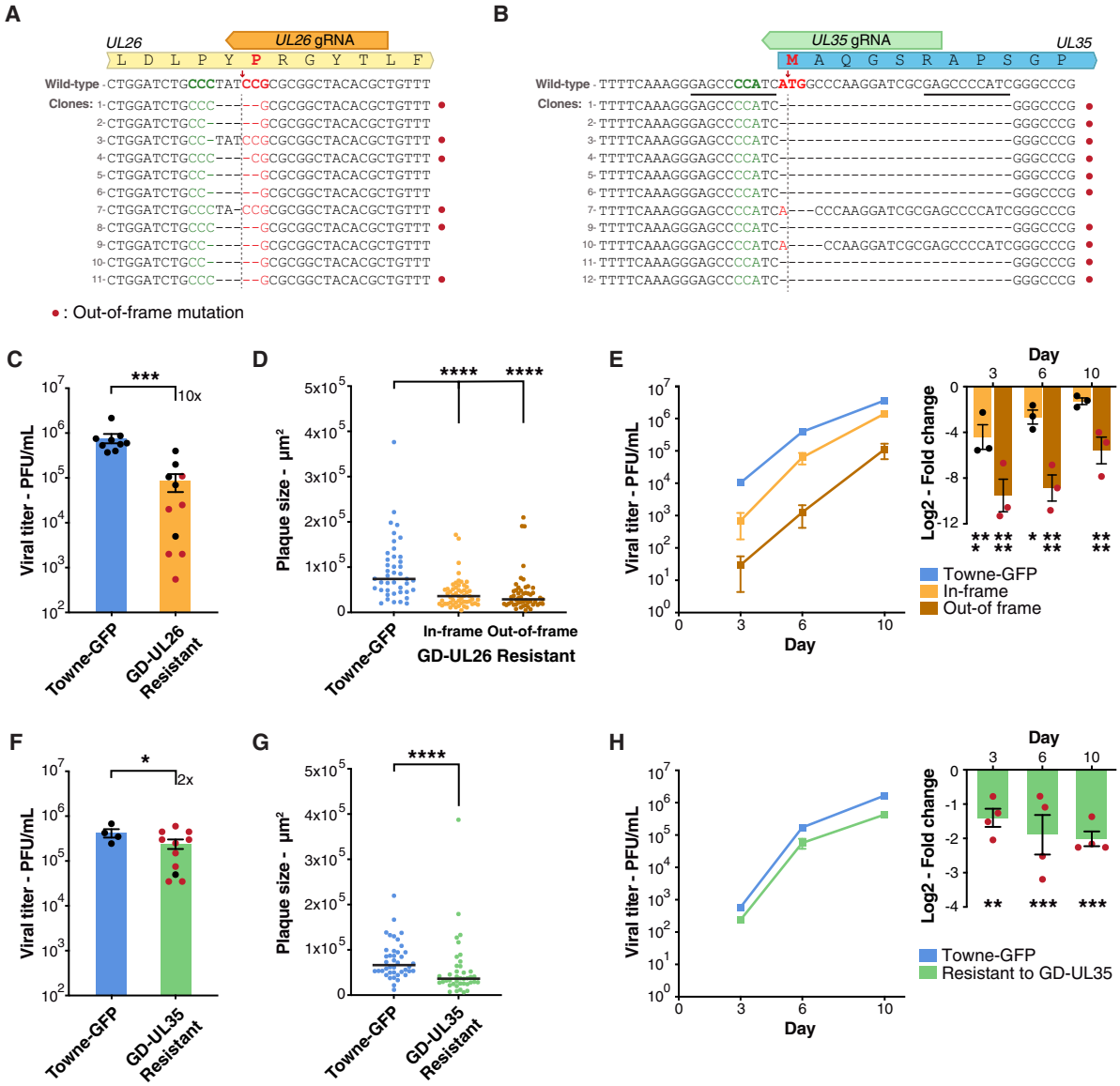


**FIG 7** Drive-resistant viruses are significantly attenuated. (A and B) Sanger sequencing of the target site of 11 viral clones resistant to either GD-UL26 (A) or GD-UL35 (B). CRISPR cleavage sites are shown by red arrows, PAMs are highlighted in green, and targeted codons are in red. Microhomology sequences around the *UL35* cleavage site are underlined in black. (C) Viral titer in fibroblasts infected with Towne-GFP or viruses resistant to GD-UL26 after 10 days. MOI = 0.1; $n = 9$ (Towne-GFP) or $n = 11$ (GD-UL26 resistant). (D) Plaque size in fibroblasts infected with Towne-GFP or viruses resistant to GD-UL26, after 7 days. Black lines indicate the median; $n = 40$ to 55. (E) Multistep growth curve after infection at an MOI of 0.1 (left) with the corresponding $\log_2$ fold change between mutants and Towne-GFP (right); $n = 3$. (F) Viral titer in fibroblasts infected with Towne-GFP or viruses resistant to GD-UL35 after 7 days. MOI = 1; $n = 4$ (Towne-GFP) or $n = 11$ (GD-UL35 resistant). (G) Plaque size in fibroblasts infected with Towne-GFP or viruses resistant to GD-UL35, after 7 days. Black lines indicate the median; $n = 45$ to 60. (H) Multistep growth curve after infection at an MOI of 0.1 (left) with the corresponding $\log_2$ fold change between mutants and Towne-GFP (right); $n = 4$. Replicates with out-of-frame mutations are highlighted in red. Data show mean and SEM between biological replicates. Asterisks summarize the results of statistical tests. *, $P < 0.05$; **, $P < 0.01$; ***, $P < 0.001$; ****, $P < 0.0001$ (C and F, Welsh *t* test on log-transformed data; D and G, Mann-Whitney or Kruskal-Wallis test; E and H, repeated-measure two-way ANOVA with Holm-Šidák's multiple-comparison test on log-transformed data).

of the long UL35 isoform. Interestingly, 9 of 11 *UL35*-resistant clones had an identical 26-bp deletion that can probably be explained by the presence of microhomology segments on both sides of the cleavage site (Fig. 7B). The viral titers of these drive-resistant viruses were then compared to that of Towne-GFP. On average, the 11 viral clones resistant to GD-UL26 were severely impaired and had a significant (10-fold) reduction of viral titers, after infection at an MOI of 0.1 ($P = 0.0003$, Welsh *t* test on log-transformed data [Fig. 7C]). To characterize in detail this replication defect, we selected

three resistant clones with in-frame (clones 5, 9, and 10) or out-of-frame (clones 3, 7, and 11) mutations. Both in-frame and out-of-frame mutants had significantly reduced plaque sizes ($P < 0.0001$, Kruskal-Wallis test [Fig. 7D]). In addition, multistep growth curves after infection at an MOI of 0.1 indicated that both in-frame and out-of-frame mutants replicated with a slower dynamic (Fig. 7E). Clones with out-of-frame mutations were severely impaired, with a 700-fold reduction at day 3 and a 45-fold reduction at day 10 ($P < 0.0001$ for the three time points, repeated-measure two-way ANOVA on log-transformed data). In-frame mutants had a more modest defect. Viral levels were significantly reduced (20- and 6-fold) after 3 and 6 days ($P = 0.002$ and 0.0119, respectively, same test as mentioned above) and remained attenuated 2-fold at day 10 ($P = 0.2134$). This result indicated that viruses resistant to GD-UL26 were significantly attenuated. Importantly, the significant defect of in-frame mutants provided an experimental confirmation that the targeted proline was important for viral fitness.

Similarly, the 11 viral clones resistant to GD-UL35 had a significant (2-fold) replicative defect compared to Towne-GFP after infection at an MOI of 1 ($P = 0.0366$, Welsh *t* test on log-transformed data [Fig. 7F]). Four resistant mutants (clones 1, 3, 4, and 5) with the same 26-bp deletion were selected for further analysis. These drive-resistant viruses had significantly reduced plaque sizes ($P < 0.0001$, Mann-Whitney test [Fig. 7G]) and replicated with a significant (2- to 4-fold) defect after infection at an MOI of 0.1 ($P = 0.0067$, 0.008, and 0.008 at days 3, 6, and 10, respectively, by repeated-measure two-way ANOVA on log-transformed data [Fig. 7H]). Altogether, these results indicated that for both GD-UL26 and GD-UL35, drive-resistant viruses were attenuated compared to Towne-GFP and had acquired long-term replicative defects.

Our results show that a strategy of designing gene drives against conserved and critical viral sequences can counterbalance the evolution of resistance. First, spread of the gene drive in the unmodified viral population caused a strong and transient reduction of viral levels. In a second phase, and even though engineered viruses did not stably persist in the viral population, remaining viruses were mutated and had acquired replicative defects, leading to a long-term reduction of viral levels.

## DISCUSSION

In this study, we analyzed the evolution of resistance in a viral gene drive against hCMV. Using multiple examples, we showed that after the successful invasion of the wild-type population, drive-resistant viruses with a mutated target site are positively selected and outcompete gene drive viruses. These numerical and experimental results mimic perfectly what was observed in insect experiments (14–16): the rapid evolution of resistance prevents the fixation of the modified sequence in the population.

Gene drives in mosquitoes generally follow one of two basic strategies: population-suppression drives aim to eliminate the targeted insect population, whereas population-replacement drives aim to replace wild populations with engineered, often pathogen-resistant, animals (35). Population-replacement drives could be imagined in viruses, in which, for example a drug-responsive gene would be introduced in the viral population, but in this study, we attempted to design population-suppression viral drives that lead to a significant reduction of viral levels. The difficulty lies in designing gene drive viruses with replicative defects that spread efficiently. Our previous study focused on a gene drive against *UL23*, a viral gene that is dispensable under normal cell culture conditions (6, 11). UL23 is involved in immunity evasion, and the replication of *UL23* mutant viruses is severely impaired by interferon gamma. We showed that a gene drive against *UL23* could still spread in the presence of interferon gamma, which gave us the first indication that a gene drive with a replicative defect could spread. In this investigation, we designed and tested gene drives against eight additional viral genes that are necessary for efficient viral infection independently of the culture condition (Table 1). We showed that gene drives against the tegument genes *UL26* or *UL35* could spread efficiently in the viral population. GD-UL35 had only a moderate replicative defect, but the GD-UL26 virus was almost noninfectious. However, coinfection

with unmodified Towne-GFP virus efficiently complemented the defective viruses and enabled their replication. The modification spread efficiently into the viral population as long as wild-type viruses were present. Once the target site had been mutated, the virus became unable to propagate further. This represents an important example for the design of suppression drives against herpesviruses.

In insects, targeting evolutionarily conserved sequences, such as the *Doublesex* gene, mitigates the appearance of drive-resistant sequences (19, 36, 37), and our approach followed similar principles. Some regions of the hCMV genome are highly variable, but others show a high degree of sequence conservation, and both *UL26* and *UL35* are reported to be among the most conserved hCMV genes (38). We designed gRNAs in regions of low genetic variation and targeted sequences encoding conserved amino acids. GD-UL26 and GD-UL35 are examples of gene drives with high and low fitness costs, respectively. As predicted by numerical simulations (Fig. 1B and Fig. 6D and E), drive-resistant viruses were selected rapidly in the gene drive against *UL26*, and GD-UL26 did not reach more than 50% of the population. In contrast, the drive against *UL35* had a higher penetrance and reached up to 80% of the population. In both cases, drive-resistant viruses had mutations that can be predicted to seriously affect the fitness of the virus. Viruses resistant to GD-UL26 had a significant growth defect compared to wild-type viruses, with both in-frame and out-of-frame mutants being attenuated (Fig. 7). The absence of *UL35* is reported to cause a modest growth defect (26), and GD-UL35-resistant viruses lacking the *UL35* start codon were slightly but significantly attenuated. Mutation of *UL35* had only a moderate effect in our cell culture experiments but would likely have important consequences *in vivo*. In summary, this work presents important proofs of principle for the design of viral gene drives. It demonstrates that both gene drive and drive-resistant viruses can have replication defects and be durably attenuated, leading to a long-term reduction of viral levels.

We aim to ultimately design similar gene drive systems that could be used to treat herpesvirus diseases. Patients infected with a herpesvirus and unable to control it could be superinfected with a gene drive virus that would reduce the infection. hCMV reactivation in immunosuppressed patients after organ transplant could be one use (39, 40). How a viral gene drive spreads *in vivo* and how the immune system reacts to superinfection will have to be studied in animal models. Our work nonetheless brings important considerations about viral dynamics. In particular, in our gene drives against *UL26* or *UL35*, viral levels dropped importantly when drive penetrance reached its maximum, with a 10- to 100-fold reduction of viral titers (Fig. 6D and E). This transient drop of viral levels could have important implications *in vivo*, as it could give the immune system a transient window to control the infection. Similarly, even a small decrease of viral fitness caused by drive-resistant mutations could have huge benefits for the infected patient. Indeed, *in vivo*, a successful gene drive would not require reducing viral levels significantly by itself but to do so just enough for the immune system to take control of the infection.

Preexisting genetic variation in hCMV or other herpesviruses would hamper the capacity of a gene drive to efficiently target wild viruses in infected patients. We designed CRISPR gRNAs in regions of low genetic diversity, but the number of available genomes (235) is small compared to the size of the hCMV population. A better assessment of the genetic diversity of herpesviruses will be necessary before a gene drive can be used against wild viruses. Nonetheless, one can envision that patients could be treated with an array of gene drive viruses, each targeting different variants or different locations. Such a strategy would increase redundancy and limit the probability that variants could escape the drive.

As a final note, the development of gene drives raises important ecological and biosafety concerns, and our approach follows the guidelines established by the NIH and the National Academy of Science (41, 42). In particular, our work was conducted using laboratory viral strains unable to infect human hosts (43) and thus eliminated risks of inadvertent release of gene drive viruses into the wild.

## MATERIALS AND METHODS

**Cells and viruses.** Human foreskin fibroblasts were obtained from the ATCC (SCRC-1041) and cultured in Dulbecco modified Eagle medium (DMEM; 10-013-CV; Corning, Corning, NY) supplemented with 10% fetal bovine serum (FBS; Sigma-Aldrich, USA) and 100 $\mu$m/liter of penicillin/streptomycin (Corning). Cells regularly tested negative for mycoplasma and were used between passages 3 and 15.

hCMV TB40/E-Bac4 (44) and Towne-GFP (T-BACwt) (20) were kindly provided by Edward Mocarski (Emory University, USA). Viral stocks were prepared and plaque assays performed exactly as reported previously (6).

Coinfection experiments were performed by coinfecting confluent fibroblasts with wild-type Towne-GFP and gene drive viruses for 1 h, with a total MOI of 0.1 to 1. Experiments were conducted using 12-well plates with 1 ml of medium per well. For time course experiments over multiple weeks, 100 to 200 $\mu$l of supernatant was used to inoculate fresh cells for 1 h before changing media, maintaining an MOI around 1 to 2 at each passage. Viral titers were measured at each passage.

For plaque size analysis, images of fluorescent viral plaques were acquired with a Nikon Eclipse Ti2 inverted microscope and Nikon acquisition software (NIS-Element AR 3.0). Plaque size in pixels was measured using ImageJ (v2.1.0) and then converted to square micrometers.

**Cloning and generation of gene drive viruses.** The gene drive construct against *UL23* was as described previously (6). The core gene drive cassette comprises a codon-optimized *SpCas9* (from *Streptococcus pyogenes*), followed by an mCherry fluorescent reporter and a U6-driven gRNA (Fig. 2A). This cassette is surrounded by homology arms specific to the site of integration. Gene drive plasmids against *UL122*, *UL79*, *UL99*, *UL55*, *UL26*, *UL35*, *UL82*, and *UL69* were built by serial modifications of the *UL23* gene drive plasmid. Briefly, homology arms and the gRNA for the *UL23* locus were removed by restriction enzyme digestion and replaced by new homology arms and gRNAs by Gibson cloning (New England BioLabs [NEB], USA), using PCR products or synthesized DNA fragments (GeneArt String fragments; Thermo Fisher, USA). GD$^{Towne}$-UL23 was generated with a gene drive plasmid targeting the *UL23* coding DNA sequence (CDS).

Cell lines stably expressing *UL26* or other viral genes were generated using lentiviral constructs. Lentivirus expression plasmids were cloned by serial modifications of Addgene plasmid 84832 (45), using digestion/ligation and Gibson cloning. The final constructs expressed the viral gene of interest, followed by in-frame puromycin and blue fluorescent protein (BFP) reporters interleaved with self-cleavable 2A peptides under the control of an EF1a promoter. Lentiviruses were produced in HEK293 cells using standard protocols as reported previously (46). Fibroblasts were then transduced with lentiviruses and selected with 1 $\mu$g/ml of puromycin for 1 week before being used (ant-pr-1; InvivoGen, USA).

Purification of gene drive viruses was performed as reported previously (6). Briefly, fibroblasts were transfected by nucleofection (kit V4XP-2024; Lonza, Switzerland) with the gene drive plasmid and infected 48 h later with Towne-GFP virus. Recombinant viruses expressing mCherry were isolated and purified by several rounds of serial dilution and plaque purification.

Viral clones resistant to either *UL26* or *UL35* gene drives were isolated by plaque purification of GFP-only viruses at the end of coinfection experiments. Ministocks were titrated by plaque assays, and the sequence of the target site was analyzed by PCR and Sanger sequencing. (UL26 primers included GGCGCGTTATAAGCACCGTGG [forward] and GCCGATGACGCGCAACTGA [reverse]; UL35 primers included ACGTCACTGGAGAACAATAAAGCGT [forward] and GGCACGCCAAAGTTGAGCAG [reverse].) Twelve resistant clones originating from 3 independent experiments were first isolated, but in both cases, only 11 could be successfully purified and sequenced.

**Amplicon sequencing.** Total DNA was extracted from infected cells with the Qiagen DNeasy kit. A 470-bp PCR product surrounding the *UL23* cut site was amplified using Phusion high-fidelity polymerase (NEB, USA) and column purified (Macherey-Nagel, Germany). Primers contained a 5′ overhang compatible with Illumina NGS library preparation. Amplicons were pooled and sequenced on an Illumina MiSeq ($2 \times 300$ paired-end) platform. Library preparation and sequencing were performed by SeqMatic (Fremont, CA). Analysis of genome editing outcomes from sequencing data was generated using the CRISPResso2 software pipeline (47). The forward primer was TCGTCGGCAGCGTCAGATGTGTATAAGAGACAGGCTTGGGGCATAAAACACCG; the reverse primer was GTCTCGTGGGCTCGGAGATGTGTATAAGAGACAGCCCAGGTACAGTTCAGACGG.

**Sequence alignment and motif analysis.** Protein sequences of the *Herpesviridae* US22 protein family were downloaded from UniProt and curated to remove duplicates. Motif discovery among the 31 protein sequences was performed using the Meme Suite 5.3.0 (http://meme-suite.org/), using the OOPS parameter and looking for motifs 10 to 30 amino acids in length (48).

Full-length genome sequences of 235 hCMV clinical and laboratory strains were downloaded from the NIAID Virus Pathogen Database and Analysis Resource (ViPR; https://www.viprbrc.org/) (49). The frequencies of variants around the CRISPR target site were calculated using simple Python and R scripts. Briefly, we recovered the sequences around the target site, using BLAST locally with the sequence of the target site as the query and the 235 hCMV sequences as the search database. Base frequencies on the aligned sequences were calculated and plotted using R packages APE v5.3 and ggplot2 v3.3.0 (50, 51).

**Statistics and reproducibility.** Plaque assay data do not satisfy the normality condition required for parametric tests, and F tests further showed that variances were often nonhomogeneous. As a consequence, statistical tests on plaque assay data were performed on log-transformed data, using statistical tests that did not assume homogeneity of the variance. Namely, we used the Welsh *t* test to compare two groups, and Welch and Brown-Forsythe ANOVA followed by Dunnett's T3 comparisons test to compare 3 or more groups. To compare multistep viral growth curves in Fig. 7, we used repeated-measure two-way ANOVA followed by Holm-Šidák's multiple-comparison test. Differences in viral plaque size

were analyzed using the Mann-Whitney or Kruskal-Wallis nonparametric test. Analyses were run using GraphPad Prism version 8.1.1 for macOS (GraphPad Software, USA). Exact *P* values are reported above.

**Numerical simulations.** Numerical simulations of viral gene drive were computed using a simplified viral replication model. Briefly, in each viral generation, N virtual cells were randomly infected and coinfected by N viruses (MOI =1), producing a new generation of viruses. In this new generation, wild-type viruses coinfected with drive viruses were converted to new gene-drive viruses or resistant viruses with a ratio of 90/10. Gene drive viruses replicate with a fitness *f*, and the coinfection rate is calculated from the MOI assuming a Poisson distribution. The code and a more thorough description are available at https://github.com/mariuswalter/ViralDrive.

**Data and code availability.** The data supporting the findings of this study are provided in this article. Amplicon sequencing data have been deposited in the Sequence Read Archive with BioProject accession no. PRJNA556897. Lentivirus expression plasmids for *UL23*, *UL122*, *UL79*, *UL99*, *UL55*, and *UL26* will be deposited in Addgene. Viruses and other reagents developed in this study are available upon request and subject to standard material transfer agreements with the Buck Institute. Any other relevant data are available upon reasonable request. Code developed for numerical simulations is available on GitHub (https://github.com/mariuswalter/ViralDrive).

## ACKNOWLEDGMENTS

We thank members of the Verdin laboratory for technical and conceptual help.

This study was funded through institutional support from the Buck Institute for Research on Aging.

M.W. designed the study. M.W. and R.P. conducted experiments. E.V. supervised and funded the project. M.W. and E.V. wrote the manuscript.

A patent application describing the use of a gene drive in DNA viruses has been filed by the Buck Institute for Research on Aging (application number PCT/US2019/034205, pending; inventor, M.W.). E.V. and R.P. declare no competing interests.

## REFERENCES

1. Pellett PE, Roizman B. 2013. Herpesviridae, p 1802–1822. *In* Knipe DM, Howley PM, Cohen JI, Griffin DE, Lamb RA, Martin MA, Racaniello VR, Roizman B (ed), Fields virology, 6th ed. Lippincott Williams & Wilkins, Philadelphia, PA.
2. Burrell CJ, Howard CR, Murphy FA. 2017. Chapter 17. Herpesviruses, p 237–261. *In* Burrell CJ, Howard CR, Murphy FA (ed), Fenner and White's medical virology, 5th ed. Academic Press, London, United Kingdom.
3. Dimmock NJ, Easton AJ. 2015. Cloned defective interfering influenza RNA and a possible pan-specific treatment of respiratory virus diseases. Viruses 7:3768–3788. https://doi.org/10.3390/v7072796.
4. Rezelj VV, Carrau L, Merwaiss F, Levi LI, Erazo D, Tran QD, Henrion-Lacritick A, Gausson V, Suzuki Y, Shengjuler D, Meyer B, Vallet T, Weger-Lucarelli J, Bernhauerová V, Titievsky A, Sharov V, Pietropaoli S, Diaz-Salinas MA, Legros V, Pardigon N, Barba-Spaeth G, Brodsky L, Saleh M-C, Vignuzzi M. 2021. Defective viral genomes as therapeutic interfering particles against flavivirus infection in mammalian and mosquito hosts. Nat Commun 12:2290. https://doi.org/10.1038/s41467-021-22341-7.
5. Tanner EJ, Kirkegaard KA, Weinberger LS. 2016. Exploiting genetic interference for antiviral therapy. PLoS Genet 12:e1005986. https://doi.org/10.1371/journal.pgen.1005986.
6. Walter M, Verdin E. 2020. Viral gene drive in herpesviruses. Nat Commun 11:4884. https://doi.org/10.1038/s41467-020-18678-0.
7. Burt A. 2003. Site-specific selfish genes as tools for the control and genetic engineering of natural populations. Proc Biol Sci 270:921–928. https://doi.org/10.1098/rspb.2002.2319.
8. Gantz VM, Jasinskiene N, Tatarenkova O, Fazekas A, Macias VM, Bier E, James AA. 2015. Highly efficient Cas9-mediated gene drive for population modification of the malaria vector mosquito Anopheles stephensi. Proc Natl Acad Sci U S A 112:E6736–E6743. https://doi.org/10.1073/pnas.1521077112.
9. Hammond A, Galizi R, Kyrou K, Simoni A, Siniscalchi C, Katsanos D, Gribble M, Baker D, Marois E, Russell S, Burt A, Windbichler N, Crisanti A, Nolan T. 2016. A CRISPR-Cas9 gene drive system targeting female reproduction in the malaria mosquito vector Anopheles gambiae. Nat Biotechnol 34:78–83. https://doi.org/10.1038/nbt.3439.
10. Champer J, Buchman A, Akbari OS. 2016. Cheating evolution: engineering gene drives to manipulate the fate of wild populations. Nat Rev Genet 17:146–159. https://doi.org/10.1038/nrg.2015.34.
11. Feng L, Sheng J, Vu G-P, Liu Y, Foo C, Wu S, Trang P, Paliza-Carre M, Ran Y, Yang X, Sun X, Deng Z, Zhou T, Lu S, Li H, Liu F. 2018. Human cytomegalovirus UL23 inhibits transcription of interferon-$\gamma$ stimulated genes and blocks antiviral interferon-$\gamma$ responses by interacting with human N-myc interactor protein. PLoS Pathog 14:e1006867. https://doi.org/10.1371/journal.ppat.1006867.
12. Dunn W, Chou C, Li H, Hai R, Patterson D, Stolc V, Zhu H, Liu F. 2003. Functional profiling of a human cytomegalovirus genome. Proc Natl Acad Sci U S A 100:14223–14228. https://doi.org/10.1073/pnas.2334032100.
13. Kalejta RF. 2008. Tegument proteins of human cytomegalovirus. Microbiol Mol Biol Rev 72:249–265. https://doi.org/10.1128/MMBR.00040-07.
14. Champer J, Reeves R, Oh SY, Liu C, Liu J, Clark AG, Messer PW. 2017. Novel CRISPR/Cas9 gene drive constructs reveal insights into mechanisms of resistance allele formation and drive efficiency in genetically diverse populations. PLoS Genet 13:e1006796. https://doi.org/10.1371/journal.pgen.1006796.
15. Hammond AM, Kyrou K, Bruttini M, North A, Galizi R, Karlsson X, Kranjc N, Carpi FM, D'Aurizio R, Crisanti A, Nolan T. 2017. The creation and selection of mutations resistant to a gene drive over multiple generations in the malaria mosquito. PLoS Genet 13:e1007039. https://doi.org/10.1371/journal.pgen.1007039.
16. Unckless RL, Clark AG, Messer PW. 2017. Evolution of resistance against CRISPR/Cas9 gene drive. Genetics 205:827–841. https://doi.org/10.1534/genetics.116.197285.
17. Noble C, Adlam B, Church GM, Esvelt KM, Nowak MA. 2018. Current CRISPR gene drive systems are likely to be highly invasive in wild populations. Elife 7:e33423. https://doi.org/10.7554/eLife.33423.
18. Drury DW, Dapper AL, Siniard DJ, Zentner GE, Wade MJ. 2017. CRISPR/Cas9 gene drives in genetically variable and nonrandomly mating wild populations. Sci Adv 3:e1601910. https://doi.org/10.1126/sciadv.1601910.
19. Marshall JM, Buchman A, Sánchez C HM, Akbari OS. 2017. Overcoming evolved resistance to population-suppressing homing-based gene drives. Sci Rep 7:3776. https://doi.org/10.1038/s41598-017-02744-7.
20. Marchini A, Liu H, Zhu H. 2001. Human cytomegalovirus with IE-2 (UL122) deleted fails to express early lytic genes. J Virol 75:1870–1878. https://doi.org/10.1128/JVI.75.4.1870-1878.2001.
21. Perng Y-C, Campbell JA, Lenschow DJ, Yu D. 2014. Human cytomegalovirus pUL79 is an elongation factor of RNA polymerase II for viral gene transcription. PLoS Pathog 10:e1004350. https://doi.org/10.1371/journal.ppat.1004350.
22. Perng Y-C, Qian Z, Fehr AR, Xuan B, Yu D. 2011. The human cytomegalovirus gene UL79 is required for the accumulation of late viral transcripts. J Virol 85:4841–4852. https://doi.org/10.1128/JVI.02344-10.

23. Silva MC, Yu Q-C, Enquist L, Shenk T. 2003. Human cytomegalovirus UL99-encoded pp28 is required for the cytoplasmic envelopment of tegument-associated capsids. J Virol 77:10594–10605. https://doi.org/10.1128/jvi.77.19.10594-10605.2003.
24. Isaacson MK, Compton T. 2009. Human cytomegalovirus glycoprotein B is required for virus entry and cell-to-cell spread but not for virion attachment, assembly, or egress. J Virol 83:3891–3903. https://doi.org/10.1128/JVI.01251-08.
25. Lorz K, Hofmann H, Berndt A, Tavalai N, Mueller R, Schlötzer-Schrehardt U, Stamminger T. 2006. Deletion of open reading frame UL26 from the human cytomegalovirus genome results in reduced viral growth, which involves impaired stability of viral particles. J Virol 80:5423–5434. https://doi.org/10.1128/JVI.02585-05.
26. Maschkowitz G, Gärtner S, Hofmann-Winkler H, Fickenscher H, Winkler M. 2018. Interaction of human cytomegalovirus tegument proteins ppUL35 and ppUL35A with sorting nexin 5 regulates glycoprotein B (gpUL55) localization. J Virol 92:e00013-18. https://doi.org/10.1128/JVI.00013-18.
27. Hayashi ML, Blankenship C, Shenk T. 2000. Human cytomegalovirus UL69 protein is required for efficient accumulation of infected cells in the G1 phase of the cell cycle. Proc Natl Acad Sci U S A 97:2692–2696. https://doi.org/10.1073/pnas.050587597.
28. Bresnahan WA, Shenk TE. 2000. UL82 virion protein activates expression of immediate early viral genes in human cytomegalovirus-infected cells. Proc Natl Acad Sci U S A 97:14506–14511. https://doi.org/10.1073/pnas.97.26.14506.
29. Munger J, Yu D, Shenk T. 2006. UL26-deficient human cytomegalovirus produces virions with hypophosphorylated pp28 tegument protein that is unstable within newly infected cells. J Virol 80:3541–3548. https://doi.org/10.1128/JVI.80.7.3541-3548.2006.
30. Stamminger T, Gstaiger M, Weinzierl K, Lorz K, Winkler M, Schaffner W. 2002. Open reading frame UL26 of human cytomegalovirus encodes a novel tegument protein that contains a strong transcriptional activation domain. J Virol 76:4836–4847. https://doi.org/10.1128/JVI.76.10.4836-4847.2002.
31. Kim YJ, Kim ET, Kim Y-E, Lee MK, Kwon KM, Kim KI, Stamminger T, Ahn J-H. 2016. Consecutive inhibition of ISG15 expression and ISGylation by cytomegalovirus regulators. PLoS Pathog 12:e1005850. https://doi.org/10.1371/journal.ppat.1005850.
32. Chee MS, Bankier AT, Beck S, Bohni R, Brown CM, Cerny R, Horsnell T, Hutchison CA, Kouzarides T, Martignetti JA, Preddie E, Satchwell SC, Tomlinson P, Weston KM, Barrell BG. 1990. Analysis of the protein-coding content of the sequence of human cytomegalovirus strain AD169. Curr Top Microbiol Immunol 154:125–169. https://doi.org/10.1007/978-3-642-74980-3_6.
33. Zheng T, Hou Y, Zhang P, Zhang Z, Xu Y, Zhang L, Niu L, Yang Y, Liang D, Yi F, Peng W, Feng W, Yang Y, Chen J, Zhu YY, Zhang L-H, Du Q. 2017. Profiling single-guide RNA specificity reveals a mismatch sensitive core sequence. Sci Rep 7:40638. https://doi.org/10.1038/srep40638.
34. Liu Y, Biegalke BJ. 2002. The human cytomegalovirus UL35 gene encodes two proteins with different functions. J Virol 76:2460–2468. https://doi.org/10.1128/jvi.76.5.2460-2468.2002.
35. Williams AE, Franz AWE, Reid WR, Olson KE. 2020. Antiviral effectors and gene drive strategies for mosquito population suppression or replacement to mitigate arbovirus transmission by Aedes aegypti. Insects 11:52. https://doi.org/10.3390/insects11010052.
36. Adolfi A, Gantz VM, Jasinskiene N, Lee H-F, Hwang K, Terradas G, Bulger EA, Ramaiah A, Bennett JB, Emerson JJ, Marshall JM, Bier E, James AA. 2020. Efficient population modification gene-drive rescue system in the malaria mosquito Anopheles stephensi. Nat Commun 11:5553. https://doi.org/10.1038/s41467-020-19426-0.
37. Kyrou K, Hammond AM, Galizi R, Kranjc N, Burt A, Beaghton AK, Nolan T, Crisanti A. 2018. A CRISPR-Cas9 gene drive targeting doublesex causes complete population suppression in caged Anopheles gambiae mosquitoes. Nat Biotechnol 36:1062–1066. https://doi.org/10.1038/nbt.4245.
38. Sijmons S, Thys K, Mbong Ngwese M, Van Damme E, Dvorak J, Van Loock M, Li G, Tachezy R, Busson L, Aerssens J, Van Ranst M, Maes P. 2015. High-throughput analysis of human cytomegalovirus genome diversity highlights the widespread occurrence of gene-disrupting mutations and pervasive recombination. J Virol 89:7673–7695. https://doi.org/10.1128/JVI.00578-15.
39. Dropulic LK, Cohen JI. 2011. Severe viral infections and primary immunodeficiencies. Clin Infect Dis 53:897–909. https://doi.org/10.1093/cid/cir610.
40. Haidar G, Singh N. 2017. Viral infections in solid organ transplant recipients: novel updates and a review of the classics. Curr Opin Infect Dis 30:579–588. https://doi.org/10.1097/QCO.0000000000000409.
41. National Academies of Sciences, Engineering, and Medicine. 2016. Gene drives on the horizon. Advancing science, navigating uncertainty, and aligning research with public values. National Academies Press, Washington, DC.
42. Emerson C, James S, Littler K, Randazzo FF. 2017. Principles for gene drive research. Science 358:1135–1136. https://doi.org/10.1126/science.aap9026.
43. Wilkinson GWG, Davison AJ, Tomasec P, Fielding CA, Aicheler R, Murrell I, Seirafian S, Wang ECY, Weekes M, Lehner PJ, Wilkie GS, Stanton RJ. 2015. Human cytomegalovirus: taking the strain. Med Microbiol Immunol 204:273–284. https://doi.org/10.1007/s00430-015-0411-4.
44. Sinzger C, Hahn G, Digel M, Katona R, Sampaio KL, Messerle M, Hengel H, Koszinowski U, Brune W, Adler B. 2008. Cloning and sequencing of a highly productive, endotheliotropic virus strain derived from human cytomegalovirus TB40/E. J Gen Virol 89:359–368. https://doi.org/10.1099/vir.0.83286-0.
45. Horlbeck MA, Gilbert LA, Villalta JE, Adamson B, Pak RA, Chen Y, Fields AP, Park CY, Corn JE, Kampmann M, Weissman JS. 2016. Compact and highly active next-generation libraries for CRISPR-mediated gene repression and activation. Elife 5:e19760. https://doi.org/10.7554/eLife.19760.
46. Vallejo-Gracia A, Chen IP, Perrone R, Besnard E, Boehm D, Battivelli E, Tezil T, Krey K, Raymond KA, Hull PA, Walter M, Habrylo I, Cruz A, Deeks S, Pillai S, Verdin E, Ott M. 2020. FOXO1 promotes HIV latency by suppressing ER stress in T cells. Nat Microbiol 5:1144–1157. https://doi.org/10.1038/s41564-020-0742-9.
47. Fu Y-Z, Su S, Gao Y-Q, Wang P-P, Huang Z-F, Hu M-M, Luo W-W, Li S, Luo M-H, Wang Y-Y, Shu H-B. 2017. Human cytomegalovirus tegument protein UL82 inhibits STING-mediated signaling to evade antiviral immunity. Cell Host Microbe 21:231–243. https://doi.org/10.1016/j.chom.2017.01.001.
48. Bailey TL, Boden M, Buske FA, Frith M, Grant CE, Clementi L, Ren J, Li WW, Noble WS. 2009. MEME Suite: tools for motif discovery and searching. Nucleic Acids Res 37:W202–W208. https://doi.org/10.1093/nar/gkp335.
49. Pickett BE, Sadat EL, Zhang Y, Noronha JM, Squires RB, Hunt V, Liu M, Kumar S, Zaremba S, Gu Z, Zhou L, Larson CN, Dietrich J, Klem EB, Scheuermann RH. 2012. ViPR: an open bioinformatics database and analysis resource for virology research. Nucleic Acids Res 40:D593–D598. https://doi.org/10.1093/nar/gkr859.
50. Paradis E, Schliep K. 2019. ape 5.0: an environment for modern phylogenetics and evolutionary analyses in R. Bioinformatics 35:526–528. https://doi.org/10.1093/bioinformatics/bty633.
51. Wickham H. 2016. ggplot2: elegant graphics for data analysis. Springer-Verlag, New York, NY.
52. Schierling K, Buser C, Mertens T, Winkler M. 2005. Human cytomegalovirus tegument protein ppUL35 is important for viral replication and particle formation. J Virol 79:3084–3096. https://doi.org/10.1128/JVI.79.5.3084-3096.2005.
53. Lischka P, Toth Z, Thomas M, Mueller R, Stamminger T. 2006. The UL69 transactivator protein of human cytomegalovirus interacts with DEXD/H-box RNA helicase UAP56 to promote cytoplasmic accumulation of unspliced RNA. Mol Cell Biol 26:1631–1643. https://doi.org/10.1128/MCB.26.5.1631-1643.2006.